Separation Science and Technology
Publication details, including instructions for authors and subscription information:
http://www.informaworld.com/smpp/title~content=t713708471

Resistance and Mass Transfer Control through Passive Porous Films. II. Applications of a Two-Dimensional Model to Salt Transport through Porous Membranes of Moderate Porosity

F. Martínez-Villa[a]; J. I. Arribas[a]; F. Tejerina[a]
[a] DEPARTAMENTO FISICA APLICADA II, FACULTAD DE CIENCIAS UNIVERSIDAD DE VALLADOLID, VALLADOLID, SPAIN

To cite this Article Martínez-Villa, F. , Arribas, J. I. and Tejerina, F.(1990) 'Resistance and Mass Transfer Control through Passive Porous Films. II. Applications of a Two-Dimensional Model to Salt Transport through Porous Membranes of Moderate Porosity', Separation Science and Technology, 25: 1, 121 — 137

To link to this Article: DOI: 10.1080/01496399008050324

URL: http://dx.doi.org/10.1080/01496399008050324

SEPARATION SCIENCE AND TECHNOLOGY, 25(1 & 2), pp. 121-137, 1990

Resistance and Mass Transfer Control through Passive Porous Films. II. Applications of a Two-Dimensional Model to Salt Transport through Porous Membranes of Moderate Porosity

---

F. MARTÍNEZ-VILLA, J. I. ARRIBAS, and F. TEJERINA

DEPARTAMENTO FISICA APLICADA II
FACULTAD DE CIENCIAS
UNIVERSIDAD DE VALLADOLID
47005 VALLADOLID, SPAIN

Abstract

In a previous study we dealt with the practical equations and the range of validity of a two-dimensional model for the diffusive flux of a solute through a membrane system. In the present study we apply the equations to the results of the experimental determination of the flux of LiCl solutions through different types of polymeric microporous membranes (Nuclepore) at several temperatures between 25 and 50°C. Thus, we have established the concentration profiles in the membrane-boundary layers interfaces, the thickness of these boundary layers, the apparent pore diffusivities, and their temperature dependence. The values of each term of the diffusive resistance have been calculated, and the relative importance of each term on the total resistance of the barrier has also been analyzed.

INTRODUCTION

The description of the mass transfer through permeable or porous barriers is usually done by means of diffusive permeability coefficients (or of diffusive resistance if a reverse formalism is used).

These types of coefficients, of relatively simple experimental determination, have the advantage—unlike molecular diffusivities—of being defined in terms of the solute concentrations in the external phases of the barrier, but not in the internal concentrations, which are not experimentally determinable. On the other hand, these coefficients include the thickness of the barrier and they are useful when the value of such a parameter is unknown *a priori (2)*.

However, these coefficients functionally characterize the barrier as a whole. So, in the case of a composite barrier they do not inform directly on the influence of each element on the permeation control, because this requires an additional hypothesis on the constitution of the former and additional experimentation.

In this paper we develop a method, applied to membrane systems, which allows us to get the aforementioned information from three types of data: a wide morphological and structural characterization of the membranes, only one type of measurement of flux based on the use of ion selective electrodes, and an adequate physical model, described in the previous paper (*1*) which will henceforth be referred to as Part I.

EXPERIMENTAL

This study has been done on five different types of polycarbonate track-etched membranes (Nuclepore) with applications in microfiltration and dialysis. Some of the results of their morphological and structural characterization were given in Table 1 of Part I.

The diffusive behavior of each one of these membranes has been studied for a long time period (8 h) in a diaphragm-type cell with stirring, and at different temperatures between 25 and 50°C. One of the compartments of the cell was supplied with an aqueous LiCl solution at a constant concentration, c_1 of 0.1 mol/L, while in the other compartment the concentration $c_2(t)$ changes to the equilibrium value under the action of diffusion through the membrane (Fig. 1). The solutions were homogenized by stirring at a moderate speed (200 rpm) in order to avoid undesirable effects (distortion of the membrane or exaggeration of the pore end effects) (*3*).

The procedure for the measurement of time variation of concentration $c_2(t)$ is a novel method consisting of continuously detecting the variations in Cl^- concentration by direct potentiometry with a selective electrode of chloride and another reference electrode (Orion 94-17 and 900-200, respectively) previously calibrated. Both electrodes are dipped in the measuring compartment (Fig. 1) and are connected to a high impedance microvoltmeter as the signal detector. A more detailed description of this procedure is given elsewhere (*4*).

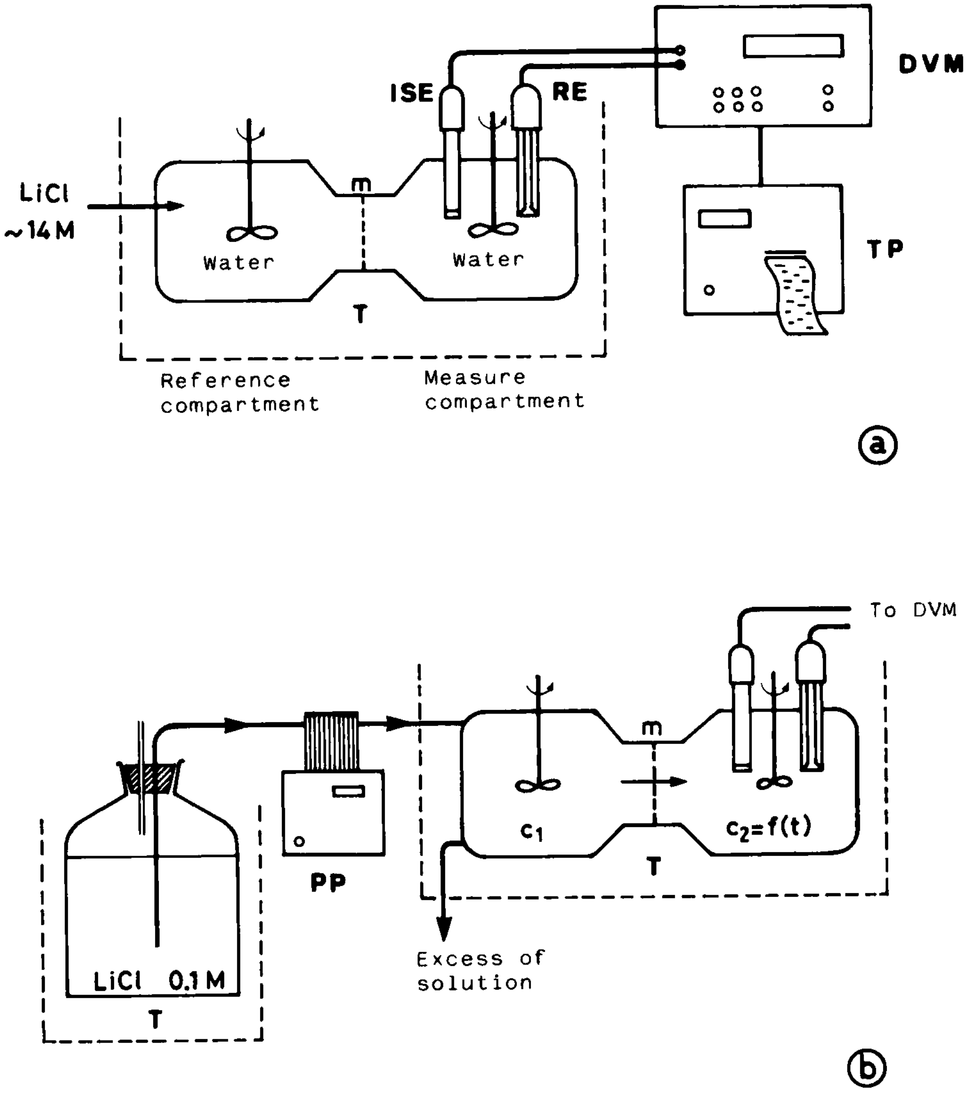

FIG. 1. Experimental device used in determination of the total diffusive permeability. (a) Set-up at the beginning of the experiment. (b) Set-up in the course of the experiment. ISE: Ion-selective electrode. RE: Reference electrode. DVM: Digital voltmeter. m: membrane. T: Thermostatic bath. TP: Thermal printer. PP: Peristaltic pump.

In each experiment the values of $c_2(t)$ are related to the overall permeability coefficient of the membrane system, P_T, by (*4*)

$$\ln\,[c_1/(c_1 - c_2)] = P_T A t / V_0 \tag{1}$$

where A is the exposed area of the membrane and V_0 is the measuring compartment volume. Equation (1) give P_T in each case from the slope of the corresponding curve c_2-t.

In Fig. 2 we present the results of P_T obtained for each type of membrane and the temperature; as can be seen, an acceptable linear correlation between the experimental points was obtained.

The relationship between P_T and the intrinsic characteristics of the membrane system (porosity, diffusivity, thickness of membranes and stagnant layer, etc.) in surface heterogeneous membranes was described in Part I. The first task in applying the practical equations of the two-dimensional model to the above experimental results is to see if the simplifications introduced are justified in this case. Thus, in the course of the experiments, geometrical and hydrodynamical similarities have been maintained on both sides of the membranes (equal volume of the cell compartments, identical stirring speed, the same solvent, etc.). As a consequence, it is reasonable to suppose the existence of a symmetry from which practically equal thicknesses of both boundary layers are derived, i.e., the identification $\delta_1 = \delta_2$ is justified.

Also, it is easy to verify that the approximation for the function $H(\beta,\lambda)$, given by Eq. (13) of Part I, i.e., $H(\beta,\lambda) = 0.250(\lambda/\beta^2) + 0.164$, which relates the geometrical and hydrodynamical parameter of the membrane system model, is valid for all the membranes studied, whose porosities are between 0.075 (membrane N01) and 0.276 (membrane N08), and their effective pore radii, r_e, which range between 0.065 μm (N01) and 2.07 μm (N5).

RESULTS AND DISCUSSION

(1) Diffusivity of the Membranes and Thickness of Boundary Layers

The main result of the model (Eq. 16 of Part I):

$$R_T = \frac{1}{\varepsilon_e D_p} + \frac{2\delta}{D\delta} + \frac{1.312}{\pi r_s N D_\delta}$$

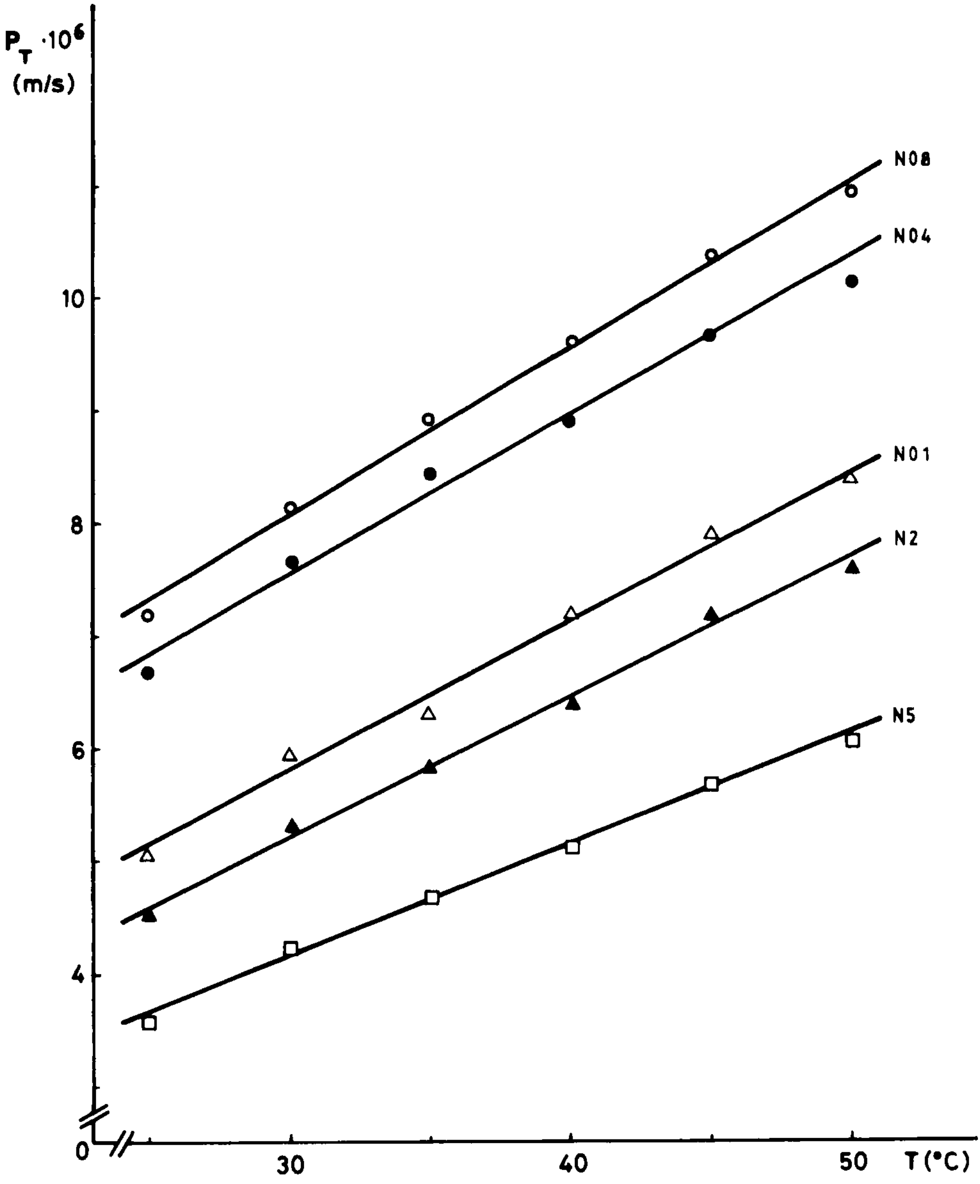

FIG. 2. Variation with temperature of the diffusive permeability for each membrane system.

suggests the existence of a linear correlation between $1/P_T$ (or R_T) and the quotient $1/\varepsilon_e$ for the group of membranes at each temperature. From the slope of each graph, a typical value of the apparent diffusivity, D_p, at the given temperature can be obtained and from the intercept, which represents the contribution $2(R_\delta + R_e)$, the thickness of the diffusion layers can be evaluated.

Bearing this in mind, a regression analysis by the least-squares method was effected. In Fig. 3 the data points are plotted with their corresponding lines of regression, while the numerical results for D_p (the inverse of the slope) and for the intercept, together with the correlation coefficient, are grouped for each fitting in Table 1.

Obtaining only one value for the pore diffusivity at each temperature is reasonable, and it is justified because the average pore radius of these membranes is always larger than the ionic radius of the permeating solute (even when it is considered to be solvated), so that steric hindrance to diffusion should be negligible. For that reason it is obvious that in this respect there are no meaningful differences for the membranes.

As for the magnitude of the values obtained for D_p, they are inferior (approximately half) to the values for the electrolyte in free diffusion at the same temperaure (*5*). This shows that these membranes are, of course, zones of restricted diffusion, but only in a moderate way if we compare them with dense membranes whose diffusivities can be 1/10 to 1/100 of the values for free diffusion. In any case, it must not be forgotten that the control that a membrane can exercise on the flux is determined, not only by the value of the diffusivity, but also by the thickness and porosity of the membrane.

We can say that D_p varies greatly with temperature, because in the range studied its value is duplicated. As we proved elsewhere (*6*), that is a thermal activation process.

In order to calculate the thickness of the diffusion layers, δ, from the intercept, we have substituted the values of r_s and ε_s obtained from microscopic analysis (Table 1, Part I). As for D_δ, we have taken it as the usual value of the diffusion coefficient of LiCl in aqueous solution at infinite dilution. This value was calculated at 25°C from ionic limiting equivalent conductances, according to the Nernst-Haskell equation (*7*), while for the remaining temperatures the following correlation was used (*8*):

$$D^\circ_{\mathrm{LiCl}}(T) = D^\circ_{\mathrm{LiCl}}(25^\circ\mathrm{C})\,\frac{T}{334\eta_a} \qquad (2)$$

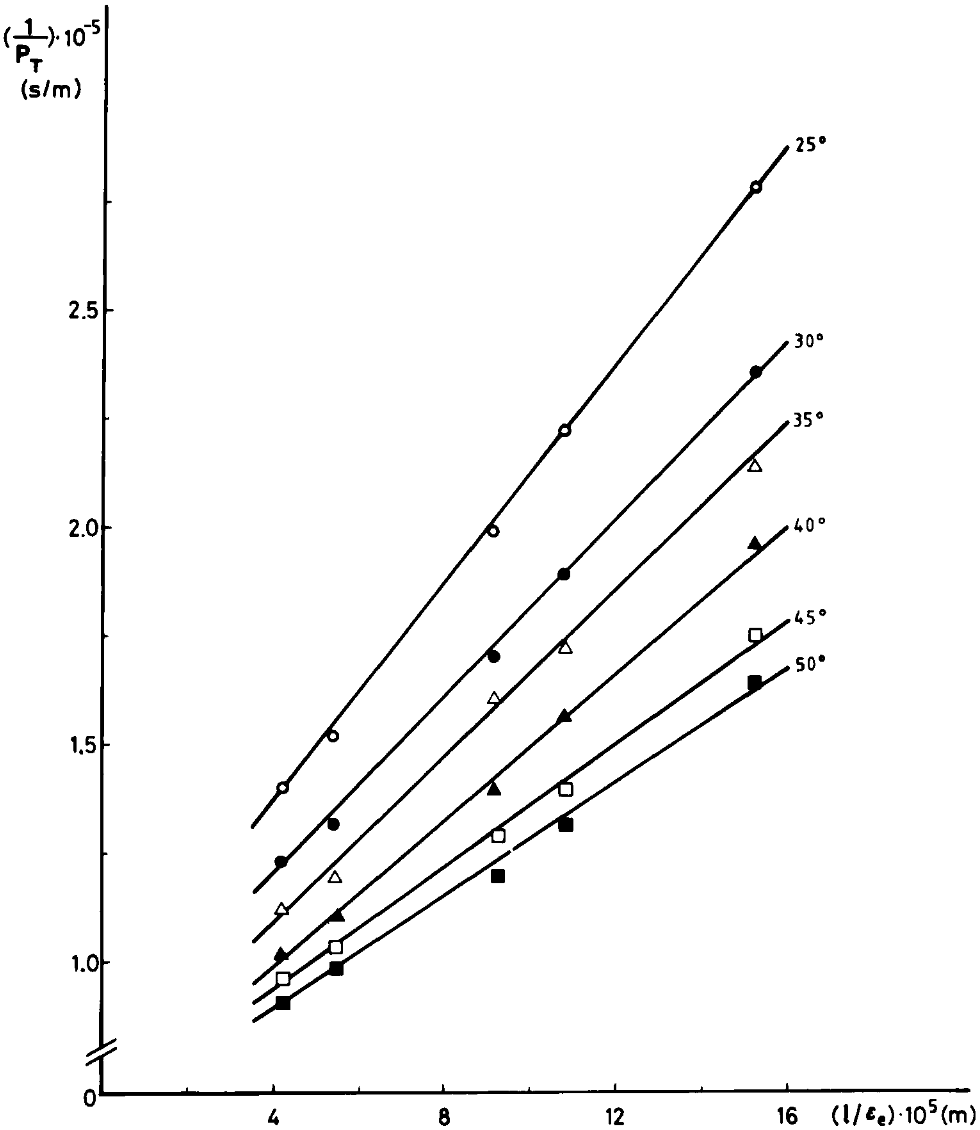

FIG. 3. Fitted values of $1/P_T$ vs $1/\varepsilon_e$ for each temperature.

TABLE 1

Results of the Linear Least-Squares Fit of $1/P_T$ vs $1/\varepsilon_e$ for All the Temperatures Studied. The Expected Errors Are Also Included in Each Case

	Temperature (°C)					
	25	30	35	40	45	50
$D_p \times 10^9$ (m^2/s)	0.79 ± 0.01	0.96 ± 0.01	1.06 ± 0.02	1.19 ± 0.01	1.40 ± 0.02	1.54 ± 0.02
$2(R_\delta + R_e) \times 10^{-4}$ (s/m)	8.46 ± 0.07	7.58 ± 0.07	7.07 ± 0.08	6.59 ± 0.06	6.41 ± 0.07	6.34 ± 0.08
Correlation coefficient	0.999	0.998	0.997	0.998	0.997	0.996

TABLE 2

Values Assigned to the Boundary Layer Diffusivities Obtained According to Eq. (2)

Temperature (°C)	25	30	35	40	45	50
$D_\delta \times 10^9$ (m²/s)	1.37	1.56	1.75	1.97	2.19	2.42

where η_a stands for the viscosity of water (in cP) at the absolute temperature T. The results of these calculations are grouped in Table 2, while estimates for the thicknesses of the boundary layers are given in Fig. 4. From these values it can be observed that the values of δ for membranes N08, N04, and N01 are practically equal, but they clearly differ from the δ values for N2 and N5.

On the other hand, in all the membranes a nonlinear increase of the parameter δ with temperature occurs. It is foreseeable that this effect is due fundamentally to the increase of D_δ with temperature as a consequence of an increase of molecular thermal motion, since the effect of variation of the kinematic viscosity is less important.

In the search for a simple correlation between δ and the temperature for each membrane, we have fitted data points to linearized forms of the functions $\delta = A \exp (B/T)$ and $\delta = A' \exp (B'T)$, where T is the absolute temperature.

As results, we obtained a better fitting for the first function with correlation coefficients of 0.99 and the following values of the parameters:

Membrane N5:

$$\ln \delta = 8.153 - (1370/T) \tag{3}$$

Membrane N2:

$$\ln \delta = 8.060 - (1253/T) \tag{4}$$

Membranes N08, N04, and N01 (averaged):

$$\ln \delta = 7.669 - (1092/T) \tag{5}$$

In Fig. 4 the experimental points and the fitted curves (continuous lines) are plotted.

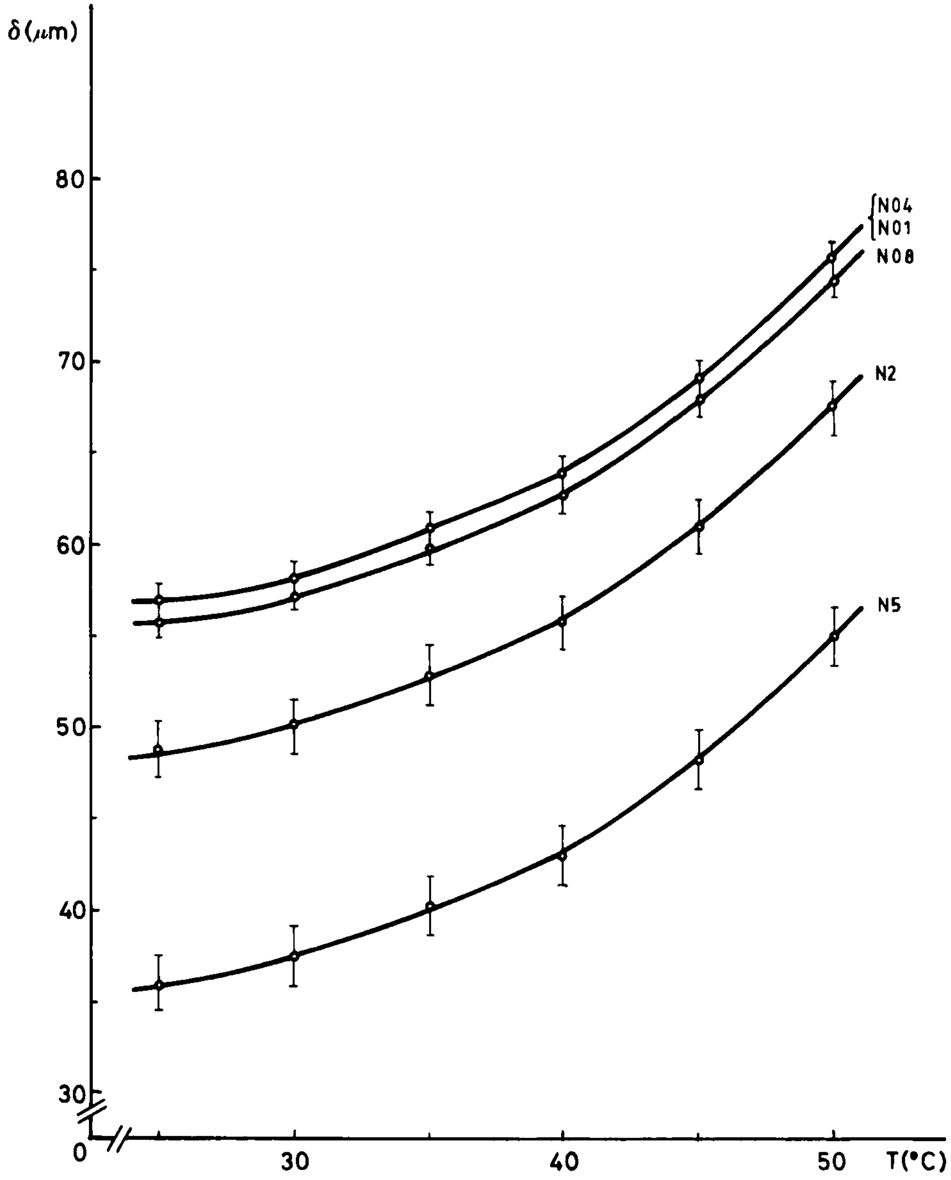

FIG. 4. Variation of the diffusion layers' thickness with temperature, the fitted lines obeying, in each case, Eqs. (3)–(5). The error bars over the data points give the expected errors in the values of the dependent variable; the errors in the independent variable can be neglected.

The results for δ belong to the range of estimated values in other studies for stirred systems. Thus Meares (*3*), using the method of Scattergood (*9*), which is based on determining the limiting current density from the characteristic current-potential curve, obtained boundary layers thicknesses around 100 μm. The same order of values was obtained by Läuger (*10*) who assumed the convective effects in the aqueous phase are moderate. But Ginzburg and Katchalsky (*11*), who based their method on the analysis of permeability through composite systems, obtained values for δ between 12 and 48 μm, depending on the membrane porosity. French (*12*) found agreement in their results on the membrane potential by assuming that δ can vary between 5 and 20 μm. On the other hand, it is possible that in unstirrred systems this thickness can reach 300–500 μm.

This wide range of values does not appear surprising if we consider that δ is an essentially hydrodynamic parameter and is therefore closely related to the experimental conditions (geometry of the cell, agitation, nature of fluids, etc.). In this sense, the estimated results obtained in the present study seem sufficiently reasonable because we are dealing with a moderately stirred system. On the other hand, the procedure used is advantageous because it does not require additional experimentation since the value of δ appears in a natural way as a consequence of the scheme for a series of diffusion resistances adopted.

(2) Interface Concentrations

By means of Eqs. (18)–(20) of Part I it is possible to calculate the values of concentrations c_1' and c_2' in the pore ends, i.e., in the membrane-boundary layer interfaces. In addition, if c_1 and c_2 are known, then the concentration profiles for each membrane system can be found.

As an example, in Fig. 5 we have plotted schematically the concentration profiles that result for the membrane systems around the N5 and N08 membranes at 25°C. For the sake of clarity, only the profiles corresponding to the beginning of each diffusion experiment, once a steady state has been attained ($c_1 = 0.1$ mol/L = constant; $c_2 \approx 10^{-4}$ mol/L) and to the end of the same experiment, when about 8 h have elapsed ($c_2 \approx 3 \times 10^{-2}$ mol/L), are included.

As can be seen, in membranes with a smaller effective porosity (such as N5), the concentration drop through the membrane itself (i.e., $c_1' - c_2'$) is larger than for membranes with a higher effective porosity (such as N08). This seems to indicate that the maintenance of a given steady flux requires a greater concentration gradient through the N5 membrane than through

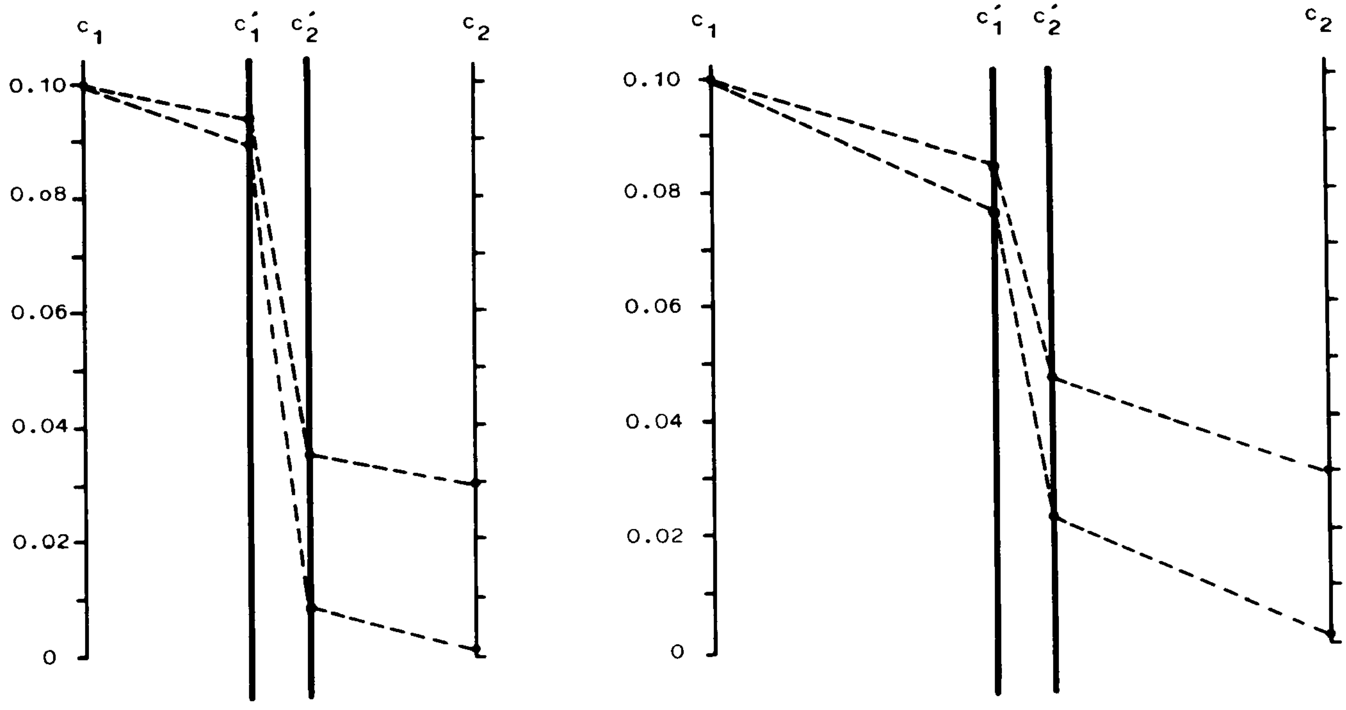

(a)

(b)

FIG. 5. Concentration profiles (dashed lines) throught the membrane system at the beginning and the end of each diffusion experiment. (a) Membrane N5, 25°C. (b) Membrane N08, 25°C. The thickness of the membranes and the adjacent boundary layers are aproximately plotted at the same scale. Concentrations are expressed in mol/L.

the N08 membrane; as a consequence, the diffusive resistance of the former is larger, as is foreseeable.

At the same time, the opposite trend can be observed in the boundary layers region, because the corresponding concentrations drops ($c_1 - c_1'$ and $c_2' - c_2$) are larger for the N08 membrane than for the N5 membrane These effects will be made more clearly evident in the next section where the diffusive resistance valued are explicity evaluated for each barrier.

(3) Relationship between Diffusive Resistances and Flux Control

It is possible to establish the influence, absolute as well as relative, that each term of the total barrier exerts on the diffusive flux. Thus, in Tables 3, 4, and 5 we present the values of the individual resistances R_m, $2R_e$, and

TABLE 3

Values of the Diffusive Resistance of the Membranes, R_m, as a Function of Temperature

	R_m (s/m)				
T (°C)	N5	N2	N08	N04	N01
25	1.93×10^5	1.38×10^5	5.28×10^4	6.90×10^4	1.16×10^5
30	1.59×10^5	1.13×10^5	4.34×10^4	5.66×10^4	9.54×10^4
35	1.44×10^5	1.03×10^5	3.93×10^4	5.14×10^4	8.66×10^4
40	1.28×10^5	0.91×10^5	3.50×10^4	4.58×10^4	7.71×10^4
45	1.08×10^5	0.77×10^5	2.96×10^4	3.87×10^4	6.51×10^4
50	0.98×10^5	0.70×10^5	2.70×10^4	3.52×10^4	5.93×10^4

TABLE 4

Values of the Diffusive Resistance Associated with the Pore End Effects as a Function of Temperature

	$2R_e$ (s/m)				
T (°C)	N5	N2	N08	N04	N01
25	3.18×10^4	1.32×10^4	2.94×10^3	1.80×10^3	1.28×10^3
30	2.79×10^4	1.16×10^4	2.59×10^3	1.58×10^3	1.13×10^3
35	2.48×10^4	1.03×10^4	2.30×10^3	1.40×10^3	1.00×10^3
40	2.21×10^4	9.22×10^3	2.05×10^3	1.25×10^3	8.93×10^2
45	1.99×10^4	8.29×10^3	1.84×10^3	1.12×10^3	8.02×10^2
50	1.79×10^4	7.49×10^3	1.66×10^3	1.02×10^3	7.25×10^2

TABLE 5
Values of the Diffusive Resistance of the Boundary Layers as a Function of Temperature

T (°C)	$2R_\delta$ (s/m)				
	N5	N2	N08	N04	N01
25	5.28×10^4	7.14×10^4	8.17×10^4	8.28×10^4	8.33×10^4
30	4.79×10^4	6.42×10^4	7.32×10^4	7.42×10^4	7.47×10^4
35	4.59×10^4	6.04×10^4	6.84×10^4	6.93×10^4	6.97×10^4
40	4.38×10^4	5.67×10^4	6.39×10^4	6.47×10^4	6.50×10^4
45	4.42×10^4	5.58×10^4	6.22×10^4	6.29×10^4	6.32×10^4
50	4.55×10^4	5.59×10^4	6.17×10^4	6.23×10^4	6.26×10^4

$2R_\delta$, respectively, calculated from their corresponding expressions arising from the model (see Eqs. 16 and 17, Part I).

On the other hand, if we consider that the total resistive contribution of the membrane phase is formed by $R_m + 2R_e$, that is, by the intrinsic contribution of the porous medium and the pore end effects, we can study the relationship between that overall term and the boundary layers resistance. Thus, it will be possible to predict the term controlling the flux in each case. In order to do this, we have elaborated in Table 6 the values of the relationship $(R_m + 2R_e)/2R\delta$ for the outermost temperatures studied (25 and 50°C); for the intermediate temperatures, the results of the quotient obviously range between the limiting values included in the table.

As can be seen, in the barrier established around membranes N5 and N2, the net influence of the mass transfer resistance of the porous media against the boundary layers increases in all temperature ranges. Accordingly, in these cases the flux is controlled by the membrane itself; this effect decreases with temperature because of the corresponding increase of the boundary layers thickness, as previously mentioned.

On the other hand, the resistance due to membranes N08 and N04 is lower than that corresponding to the stagnant films, which are thus converted in the flux controlling strata. For the same above-mentioned reason, the effect of the boundary layers also increases with temperature. Finally, for membrane N01 at 25°C, a certain influence of control by the membrane is present; this effect decreases progressively with temperature, becoming equivalent to the boundary layers effect at 50°C. It is foreseeable that if the temperature were increased, an inversion of the control would be produced, as has been pointed out for other membranes (*13*).

TABLE 6
Values of the Dimensionless Ratios $(R_m + 2R_e)/2R_\delta$ and $2R_e/R_m$ for All the Membrane Systems Studied as a Function of the Extremes of Temperature

	$(R_m + 2R_e)/2R_\delta$		$2R_e/R_m$	
Membrane	25°C	50°C	25°C	50°C
N5	4.3	2.6	0.17	0.18
N2	2.1	1.4	0.10	0.11
N08	0.7	0.5	0.06	0.06
N04	0.9	0.6	0.03	0.03
N01	1.4	1.0	0.01	0.01

Therefore, it must be emphasized that in the case of composite barriers such as those studied here, it is not enough to identify the term which is exerting kinetic control under the given conditions. It is also necessary to recognize that this control can be transferred from one term to another term of the barrier, depending on the variations undergone by the process variables.

On the other hand, it is also interesting to consider the relative importance of the pore end resistance against the intrinsic resistance of the membrane in order to determine if R_e may be an appreciable quantity with respect to R_m or, on the contrary, if it can be neglected. In Table 6 we group the results of this relationship for the outermost temperatures. From the results it can be deduced that, since the pore end effects in membranes N01 and N04 represent approximately 1 and 3%, respectively, of the total membrane resistance (which is related to the relatively high value reached by the pore length/pore diameter ratio for these membranes), we can consider such a class of effects to be negligible (*14*, *15*), and the one-dimensional approximation of the problem can be considered sufficient. Nevertheless, in the rest of the membranes the term $2R_e$ is an appreciable part of R_m (in membrane N5, about 18%); consequently, in this case and in similar ones, it is not reasonable to omit its influence, and the practical equations of the two-dimensional model can provide a suitable estimation method.

CONCLUSION

Experiments on the diffusive permeation of LiCl solutions through some Nuclepore porous membranes have been interpreted by the proposed permeation model in which the diffusion processes, both in the aqueous stagnant film and the membrane pore, and the effects associated with the pore end, were taken into account.

We think that the approach described in this work can be useful in technological, medical, and pharmaceutical applications of porous membranes (dialysis, electrodialysis, diffusion through battery separators, drug-controlled release, etc.) as well as in other fields which do not strictly pertain to membranes (for example, catalysis or evaporation through tissues) but in which mass transfer through a porous material takes place. The reason for this is that in all of the mentioned processes, the principal underlying mechanism (sometimes the only one) is the diffusive permeation of a given species.

Acknowledgment

The authors are indebted to the Caja de Ahorros de Salamanca, Spain, for financial assistance.

REFERENCES

1. F. Martínez-Villa, J. I. Arribas, and F. Tejerina, *Sep. Sci. Technol.*, *25*, 109 (1990).
2. S. Hwang and K. Kammermeyer, *Membrane in Separation*, Krieger, Florida, 1984, Chap. 1.
3. P. Meares and K. R. Page, "Rapid Force-Flux Transitions in Highly Porous Membranes," *Philos. Trans. R. Soc.*, *272*, 1 (1972).
4. F. Martínez-Villa, L. Martínez, J. I. Arribas, and F. Tejerina, "Effects of Structure and Charge on the Diffusive Salt Permeation across Microporous Membrane Filters," *J. Membr. Sci.*, *36*, 31 (1988).
5. J. O'M. Bockris and A. K. M. Reddy, *Modern Electrochemistry*, Vol. 1, Plenum, New York, 1970.
6. F. Martínez Villa, Thesis, Universidad de Valladolid, Valladolid, Spain, 1987.
7. R. Robinson and R. Stokes, *Electrolyte Solutions*, Butterworths, London, 1959.
8. R. Reid, J. Prausnitz, and T. K. Sherwood, *Properties of Gases and Liquids*, McGraw-Hill, New York, 1977.
9. E. Scattergood and E. Lightfoot, "Diffusive Interaction in Ionic Exchange Membranes," *Trans. Faraday Soc.*, *64*, 1135 (1968).
10. P. Läuger, J. Richter, and W. Lesslauer, "Electrochemistry of Biomolecular Phospholipid Membranes," *Ber. Bunsenges. Phys. Chem.*, *71*, 906 (1967).
11. B. Ginzburg and A. Katchalsky, "The Frictional Coefficients of the Flows of Non-Electrolytes through Artificial Membranes," *J. Gen. Physiol.*, *47*, 403 (1963).
12. R. French, "Unstirred Layer Effects on Calculations of the Potential Difference across an Ion Exchange Membrane," *Biophys. J.*, *18*, 53 (1977).

13. G. Flynn, A. French, N. Ho, W. Higuchi, E. Ostafin, L. Warbasse, G. Amidon, and E. Williams, "Some Hydrodynamics Boundary Layer Influences on Mass Transfer Coefficients," *J. Membr. Sci.*, *19*, 289 (1984).
14. G. Flynn and S. Yalkowsky, "Correlation and Prediction of Mass Transport across Membranes," *J. Pharm. Sci.*, *61*, 838 (1972).
15. S. Roy, E. Ruckenstein, and P. Stroeve, "Diffusion of a Nonionic Surfactant through Polymeric Membranes," *J. Colloid Interface Sci.*, *92*, 383 (1983).

Received by editor March 8, 1989